

Proceedings of the Second United Nations International Conference on the Peaceful Uses of Atomic Energy

Held in Geneva

1 September - 13 September 1958

Volume 6

Basic Metallurgy and Fabrication of Fuels



A/CONF.15/1 English, Vol. 6

UNITED NATIONS PUBLICATION

Sales No.: 58. IX. 2. Vol. 6

Price : \$U.S. 18.00; £6 9s. (stg.) ; Sw. fr. 77.00
(or equivalent in other currencies)

PRINTED IN GREAT BRITAIN

PREFACE

More than 2,100 papers were submitted by the nations, the specialized agencies, and the International Atomic Energy Agency, which participated in the Second United Nations International Conference on the Peaceful Uses of Atomic Energy. The number of papers was thus about twice that involved in the First Conference. Provision was therefore made to hold five concurrent technical sessions in comparison with the three that were held in 1955. Even so, the percentage of orally presented papers was less in 1958 than in 1955.

In arranging the programme, the Conference Secretariat aimed at achieving a balance, allowing adequate time for presentation of as many papers as possible and, nevertheless, leaving time for discussion of the data presented. Three afternoons were left free of programme activities so that informal meetings and discussions among smaller groups could be arranged. No records of these informal meetings were made.

A scientific editorial team assembled by the United Nations checked and edited all of the material included in these volumes. This team consisted of: Mr. John H. Martens, Miss L. Ourom, Dr. Walter M. Barss, Dr. Lewis G. Bassett, Mr. K. R. E. Smith, Martha Gerrard, Mr. F. Hudswell, Betty Guttman, Dr. John H. Pomeroy, Mr. W. B. Woollen, Dr. K. S. Singwi, Mr. T. E. F. Carr, Dr. A. C. Kolb, Dr. A. H. S. Matterson, Mr. S. Peter Welgos,

Dr. I. D. Rojanski, Dr. David Finkelstein, Dr. Cavid Erginsoy (Dr. Erginsoy's services were furnished through the courtesy of the International Atomic Energy Agency) and Dr. Vera J. Peterson, Dr. Paul S. Henshaw and Dr. Hywell G. Jones.

The speedy publication of such a vast bulk of literature obviously presents considerable problems. The efforts of the editors have therefore been primarily directed towards scientific accuracy. Editing for style has of necessity been kept to a minimum, and this should be noted particularly in connection with the English translations of certain papers from French, Russian and Spanish.

The Governments of the Union of Soviet Socialist Republics and of Czechoslovakia provided English translations of the papers submitted by them. Similarly, the Government of Canada provided French-language versions of the Canadian papers selected for the French edition. Such assistance from Governments has helped greatly to speed publication.

The task of printing this very large collection of scientific information has been shared by printers in Canada, France, Switzerland, the United Kingdom and the United States of America.

The complete Proceedings of the Second United Nations International Conference on the Peaceful Uses of Atomic Energy are published in a 33-volume English-language edition as follows:

Volume No.	Sessions Included
1 Progress in Atomic Energy	1, 2, 23a, 23b, 23c
2 Survey of Raw Material Resources	E-5, E-7b, E-9
3 Processing of Raw Materials	E-10, E-6 and E-7a
4 Production of Nuclear Materials and Isotopes	E-11, E-12, C-14, C-15
5 Properties of Reactor Materials	E-14, E-15
6 Basic Metallurgy and Fabrication of Fuels	E-13, E-17, E-18
7 Reactor Technology	E-19, E-21, E-22
8 Nuclear Power Plants, Part 1	3, 6, 7
9 Nuclear Power Plants, Part 2	B-9, B-10, B-11
10 Research Reactors	B-5, B-12
11 Reactor Safety and Control	B-13, B-14a, A-14
12 Reactor Physics	B-17, B-18, B-21
13 Reactor Physics and Economics	B-19, B-15, B-14b
14 Nuclear Physics and Instrumentation	A-18, A-19
15 Physics in Nuclear Energy	A-21, A-22

<i>Volume No.</i>		<i>Sessions Included</i>
16	Nuclear Data and Reactor Theory	A-11, A-12, A-13
17	Processing Irradiated Fuels and Radioactive Materials	C-17, C-18, C-19
18	Waste Treatment and Environmental Aspects of Atomic Energy	C-21, C-22, D-19
19	The Use of Isotopes: Industrial Use	5b, D-7
20	Isotopes in Research	D-6
21	Health and Safety: Dosimetry and Standards	5a, D-15
22	Biological Effects of Radiation	D-9, D-10
23	Experience in Radiological Protection	D-11, D-12
24	Isotopes in Biochemistry and Physiology, Part 1	D-13
25	Isotopes in Biochemistry and Physiology, Part 2	D-14
26	Isotopes in Medicine	D-17, D-18
27	Isotopes in Agriculture	D-21, D-22
28	Basic Chemistry in Nuclear Energy	C-9, C-10, C-11
29	Chemical Effects of Radiation	C-12, C-13
30	Fundamental Physics	15, A-17
31	Theoretical and Experimental Aspects of Controlled Nuclear Fusion.....	4, A-5, A-6
32	Controlled Fusion Devices	A-7, A-9, A-10
33	Index of the Proceedings	

TABLE OF CONTENTS

Volume 6

Session E-13: Basic Studies in Metallurgy and Ceramics

	Uranium	Page
P/1258	Lacombe, Calais..... Growth of Large Perfect Uranium Crystals.....	3
P/1855	Bierlein, Mastel Metallographic Studies of Uranium.....	14
P/2307	Sergeyev <i>et al.</i> Fabrication and Properties of Uranium.....	25
P/1324	Hasiguti, Kiyoura Physical Metallurgy of Nuclear Fuels	34
P/27	Jepson <i>et al.</i> Transformation Behaviour of Dilute Uranium Alloys..	42
P/618	Seigle, Castleman Irradiation Damage in Uranium	55
P/619	Bleiberg Radiation Damage in Uranium-Base Alloys	60
P/2306	Bochvar <i>et al.</i> Self-Diffusion of Uranium in the Gamma Phase	68
P/1160	Adda, Philibert Diffusion of Uranium with Transition Metals.....	72
P/1097	Myers, Robins Production of Uranium-Alloy Powders.....	91
P/1443	Kieffer, Sedlatschek Infiltrated Uranium Alloys	96
P/1469	Howlett, Knapton U-Ti, U-Zr and U-Ti-Zr Alloy Systems.....	104
P/789	Merten <i>et al.</i> Zirconium-Uranium-Hydrogen Alloys	111
P/710	Albrecht, Koehl Reactivity of Uranium Compounds in Gases	116
P/1474	Brabers..... Electrical Conductivity of Uranium Oxides.....	122
P/2193	Budnikov <i>et al.</i> Binary Phase Diagrams.....	124
	Thorium	
P/1705	Kantan <i>et al.</i> Sintering of Thorium and Thoria.....	132
P/2043	Ivanov, Badajeva Ternary Systems of Uranium and Thorium.....	139
P/706	Bentle Thorium-Uranium Alloy System.....	156
	Plutonium	
P/71	Waldron <i>et al.</i> Physical Metallurgy of Plutonium.....	162
P/1030	Nelson, Thomas Transformation Kinetics of Plutonium.....	170
P/327	Abramson <i>et al.</i> Properties of Plutonium and its Al Alloy.....	174
P/2197	Bochvar <i>et al.</i> Interaction of Plutonium and Other Metals.....	184
P/2230	Konobeevsky <i>et al.</i> Physical Properties of Uranium and Plutonium.....	194
P/699	Waber Corrosion of Plutonium and Uranium.....	204
P/701	Holley <i>et al.</i> Thermodynamics and Phase Diagrams of Pu Oxides....	215
	Miscellaneous	
P/2490	Voronov <i>et al.</i> Phase Diagrams for $\text{UO}_2\text{-ZrO}_2$ and $\text{ThO}_2\text{-ZrO}_2$	221
P/1866	Lillie Effects of Gases in Metallic Lattices.....	226
P/709	Markowitz Thermal Diffusion of Hydrogen in Zircaloy-2	235



		<i>Page</i>
P/1714	Hoffmann.....	Attaining the Superheated State..... 240
P/1712	Pal.....	Theory of Lattice Disturbances due to Neutrons..... 245
P/998	Seeger	Theory of Radiation Damage and Hardening..... 250
P/2385	Holmes <i>et al.</i>	Radiation Effects in Noble Metals 274
P/2042	Shatalov, Nikitina	Corrosion of Metals in Ionized Air 284
P/1366	Fumi.....	Point Imperfections in the Alkali Halides..... 288
P/712	Klopp <i>et al.</i>	Kinetics of Oxidation of Niobium Alloys..... 293
P/1293	Bally, Benes.....	Structure of Irradiated Fe-Ni Alloys..... 307
	Record of session	309

Session E-17: Fabrication of Fuels, Part I

Uranium Metal

P/317	Butler <i>et al.</i>	Manufacture of Calder Hall Fuel Element..... 317
P/1157	Stohr <i>et al.</i>	Fuel Elements in Pressurized-Gas Reactors 324
P/1161	Briola	Automatic Welding of Fuel Elements..... 343
P/1433	Fellows	Production Forming of Uranium..... 352
P/1523	Wootton, Dennis.....	Hunterston Fuel Element..... 362
P/2053	Khristenko <i>et al.</i>	Rod Fuel Element for Gas-Cooled Heavy-Water Power Reactor..... 370
P/240	Bodmer <i>et al.</i>	Manufacture of Internally-Cooled Uranium Fuel Elements 379
P/1889	Cuthbert <i>et al.</i>	Low-Enrichment-Uranium Fuel-Element Cores 384
P/2378	McGonnagle, Paul	Nondestructive Testing of Fuels 389

Uranium Alloys

P/713	Chiswik <i>et al.</i>	Physical Metallurgy of Uranium and its Alloys..... 394
P/49	McIntosh, Heal	Properties of Uranium and its Alloys..... 410
P/1470	Lloyd, Williams	Powder Metallurgy of Uranium..... 423
P/785	Hayward, Corzine	Thorium-Uranium Fuel Elements for SRE..... 438
P/790	Macherey	Uranium-Base Fuel Plates for EBWR 443
P/1004	Boettcher <i>et al.</i>	Fuel Elements in the Karlsruhe Research Reactor FR-2 449
P/1402	Cesoni <i>et al.</i>	Burnable Poisons in Aluminum-Uranium Alloys..... 451
P/1167	Stohr <i>et al.</i>	Fuel Elements for EL3 463
P/787	Turnbull <i>et al.</i>	Seed Fuel Elements for PWR 481
P/44	Turner, Williams.....	Fuel Elements for Dounreay Fast Reactor..... 486
P/791	Noland <i>et al.</i>	EBR-I Mark-III Fuel and Blanket Rods..... 501
P/792	McDaniel <i>et al.</i>	Core Elements for Enrico Fermi Power Reactor..... 509

Uranium Ceramics and Dispersion-Type Elements

P/784	Shapiro, Galvez	Stainless Steel and Oxide Dispersion Fuel..... 516
P/1925	Cunningham, Beaver.....	APPR Fuel Technology..... 521
P/1585	Mazza	The Manufacture of Fuel Elements of the Argonaut Type 531
P/318	Murray, Williams	Ceramic and Cermet Fuels..... 538
P/1162	Dubuisson <i>et al.</i>	Uranium-Uranium Carbide Cermets..... 551
P/964	Boettcher, Schneider	Some Properties of Uranium Monocarbide..... 561
	Record of session	564

Session E-18: Fabrication of Fuels, Part II

Page

Uranium Oxide Fuel

P/2404	Belle	Properties of Uranium Dioxide.....	569
P/192	Chalder <i>et al.</i>	Fabrication and Properties of UO ₂ Fuel.....	590
P/142	Runfors <i>et al.</i>	The Sintering of Uranium Dioxide.....	605
P/1165	Bel, Carteret	Sintering of Uranium Dioxide	612
P/2368	Terraza <i>et al.</i>	Sintering UO ₂ at Medium Temperatures.....	620
P/182	Schönberg <i>et al.</i>	Uranium Dioxide Compacts for Fuel Elements	624
P/2380	Glatte <i>et al.</i>	PWR Blanket Fuel Elements	630
P/2196	Ambartsumyan <i>et al.</i>	Fuel Elements for Water-Cooled Reactors	645
P/193	Robertson <i>et al.</i>	Behaviour of Uranium Oxide as a Reactor Fuel.....	655
P/615	Barney	Irradiation Effects in UO ₂	677

Plutonium Fuel

P/1046	Coffinberry <i>et al.</i>	Physical Metallurgy of Plutonium and its Alloys.....	681
P/1081	Gardner <i>et al.</i>	Tensile Properties of Pu and Pu-Al Alloys.....	686
P/1452	Waldron <i>et al.</i>	Plutonium Technology for Reactors.....	690
P/546	Lyon	Preparing and Reprocessing Pu-Al Alloy.....	697
P/1776	Wick <i>et al.</i>	Plutonium Fuels Development.....	700
P/191	Runnalls	Irradiation of Rods of Plutonium-Aluminum Alloy....	710
Record of session.....			718

Session E-13

BASIC STUDIES IN METALLURGY AND CERAMICS

LIST OF PAPERS

	<i>Uranium</i>	<i>Page</i>
P/1258	The growth of large perfect crystals of uranium by cold working and annealing polygonized crystals obtained by beta-alpha phase transformation.....P. Lacombe and D. Calais	3
P/1855	Metallographic studies of uranium.....T. K. Bierlein and B. Mastel	14
P/2307	The influence of fabrication methods on the structure and properties of uranium.....G. Y. Sergeyev <i>et al.</i>	25
P/1324	Fundamental researches on the physical metallurgy of nuclear fuels in Japan.....R. R. Hasiguti and R. Kiyoura	34
P/27	Transformation behaviour of some dilute uranium alloys.....M. D. Jepson <i>et al.</i>	42
P/618	Mechanism of irradiation-induced dimensional instability of uranium.....L. L. Seigle and L. S. Castleman	55
P/619	Irradiation-induced phase changes in uranium-base alloys.....M. L. Bleiberg	60
P/2306	Self-diffusion of uranium in the gamma phase.....A. A. Bochvar <i>et al.</i>	68
P/1160	Diffusion of uranium with some transition metals.....Y. Adda and J. Philibert	72
P/1097	Uranium-alloy powders by direct reduction of oxides.....R. H. Myers and R. G. Robins	91
P/1443	Uranium alloys prepared by the powder-metallurgical infiltration process.....R. Kieffer and K. Sedlatschek	96
P/1469	The uranium-titanium, uranium-zirconium and uranium-titanium-zirconium alloy systems.....B. W. Howlett and A. G. Knapton	104
P/789	The preparation and properties of zirconium-uranium-hydrogen alloys.....U. Merten <i>et al.</i>	111
P/710	Reactivity of uranium compounds in several gaseous media....W. M. Albrecht and B. G. Koehl	116
P/1474	Electrical conductivity of uranium oxides.....M. J. Brabers	122
P/2193	Binary phase diagrams for $\text{UO}_2\text{-Al}_2\text{O}_3$, $\text{UO}_2\text{-BeO}$ and $\text{UO}_2\text{-MgO}$P. P. Budnikov <i>et al.</i>	124
	<i>Thorium</i>	
P/1705	Sintering of thorium and thoria.....S. K. Kantan <i>et al.</i>	132
P/2043	Phase diagrams of certain ternary systems of uranium and thorium.....V. E. Ivanov and T. A. Badajeva	139
P/706	Study of the thorium-uranium alloy system.....G. G. Bentle	156

LIST OF PAPERS

(Continued)

	<i>Plutonium</i>	<i>Page</i>
P/71	The physical metallurgy of plutonium.....M. B. Waldron <i>et al.</i>	162
P/1030	Transformation kinetics of plutonium.....R. D. Nelson and I. D. Thomas	170
P/327	Some properties of plutonium and aluminum-plutonium alloy.....R. Abramson <i>et al.</i>	174
P/2197	Interaction of plutonium and other metals in connection with their arrangement in Mendeleev's Periodic Table.....A. A. Bochvar <i>et al.</i>	184
P/2230	Some physical properties of uranium, plutonium and their alloys.....S. T. Konobeevsky <i>et al.</i>	194
P/699	The corrosion behavior of plutonium and uranium.....J. T. Waber	204
P/701	Thermodynamics and phase relationships for plutonium oxides.....C. E. Holley Jr. <i>et al.</i>	215
	 <i>Miscellaneous</i>	
P/2490	Phase-equilibrium diagrams of the $\text{UO}_2\text{-ZrO}_2$ and $\text{ThO}_2\text{-ZrO}_2$ systems.....N. M. Voronov <i>et al.</i>	221
P/1866	Effects of pseudo-fission gases in metallic lattices.....D. W. Lillie	226
P/709	The thermal diffusion of hydrogen in Zircaloy-2.....J. M. Markowitz	235
P/1714	Possibility of attaining the superheated solid state in reactors.....T. A. Hoffmann	240
P/1712	Statistical theory of solid-body lattice disturbances after bombardment by fast neutrons.....L. Pal	245
P/998	On the theory of radiation damage and radiation hardening.....A. K. Seeger	250
P/2385	On the interpretation of radiation effects in the noble metals.....D. K. Holmes <i>et al.</i>	274
P/2042	Corrosion behaviour of structural metals in ionized air.....I. V. Shatalov and V. A. Nikitina	284
P/1366	Point imperfections in the alkali halides.....F. G. Fumi	288
P/712	Effects of alloying on the kinetics of oxidation of niobium.....W. D. Klopp <i>et al.</i>	293
P/1293	Study of the absorption discontinuities of X-rays and of the crystallographic structure of some iron-nickel alloys irradiated by neutrons.....D. Bally and L. Benes	307

The Growth of Large Perfect Crystals of Uranium by Cold Working and Annealing Polygonized Crystals obtained by Beta-Alpha Phase Transformation

By Paul Lacombe and Daniel Calais*

The only way in which it has been possible heretofore to prepare large uranium crystals of the non-polygonized type has been by using the phenomenon of discontinuous growth of the grain in the presence of a dispersed phase.¹ This is a method inspired by Beck's research on the exaggerated growth of grains in alloys of Al, Mn and Cu.² The conventional technique of critical cold-working, applied to polycrystalline samples with a fine grain, causes the development of crystals which are perfect but is limited to small dimensions (1 to 2 mm diam), despite all the effort of various research workers^{1, 3} to increase their size. The heterogeneity of the plastic deformation undergone by the crystals of the polycrystalline aggregate, due to the multiplicity of the modes of deformation of the uranium, must be a first explanation for the failure of the critical cold working method.

It has been thought, therefore, that it would be easier to define critical cold-working by applying it to imperfect monocrystals, namely, polygonized ones, such as can be obtained by the $\beta \rightarrow \alpha$ phase-shift method.³⁻⁵ Indeed, it is likely that the deformation of

the imperfect monocrystals would be more homogeneous in the total mass of the crystal, due to a lack of interaction between neighboring crystals. In the second place, it is easier to define the mechanism of plastic deformation as a function of the orientation of the crystal most favorable to the formation of nuclei for recrystallization.

Our study is divided into four main parts: (a) preparation of imperfect crystals by phase shift; (b) study of plastic deformation by strain as a function of the orientation of the crystal, comparing the changes in the micrographic structure with those noted on the strain curve; (c) relationship between plastic deformation and the evolution of its structure by annealing above the α -phase stability range, and (d) optimum conditions for the growth of large perfect grains of α -uranium.

RESULTS

Preparation of Imperfect Monocrystals by Phase Shift

The conventional method³⁻⁵ consists of slowly cooling a rolled strip of metal by moving it in a temperature gradient, such that passage from the β to the α phase should take place over the whole sample by local contact. We used as large a temperature gradient as possible within the temperature range of the furnace. This high gradient makes it possible to minimize the shift in the isothermal front, along the metal strip, due to small oscillations in the thermal adjustment of the furnace. A variation of $\pm 1^\circ\text{C}$ thus causes a shift of the $\beta \rightarrow \alpha$ isotherm by only 0.2 mm if the temperature gradient is $120^\circ\text{C}/\text{cm}$.

This gradient may be slightly modified according to the cross-section of the sample subjected to growth, because of the variation in the heat capacity of the sample. For instance, for samples having a cross-section 0.5 to $1 \text{ mm} \times 5 \text{ mm}$, a $120^\circ\text{C}/\text{cm}$ gradient was used and, for a cross section of $3 \text{ mm} \times 5 \text{ mm}$, the gradient was reduced to $70^\circ\text{C}/\text{cm}$ (Fig. 1). The optimum translational speed for the growth of monocrystals may vary between 0.5 and 3 mm/hr .

Previous passage of the samples into the γ phase is not a necessary condition for the growth of single crystals. It only makes it easier to obtain a higher gradient in the $\beta \rightarrow \alpha$ treatment. The length of the

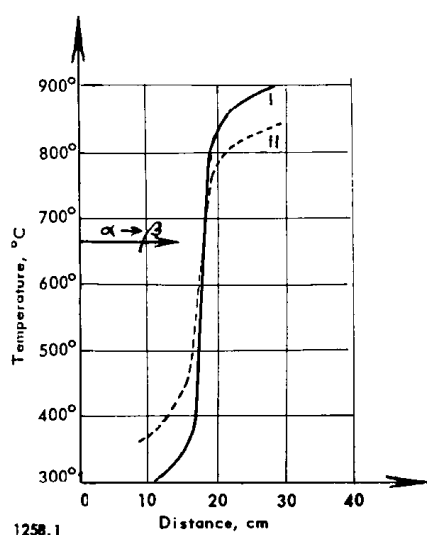
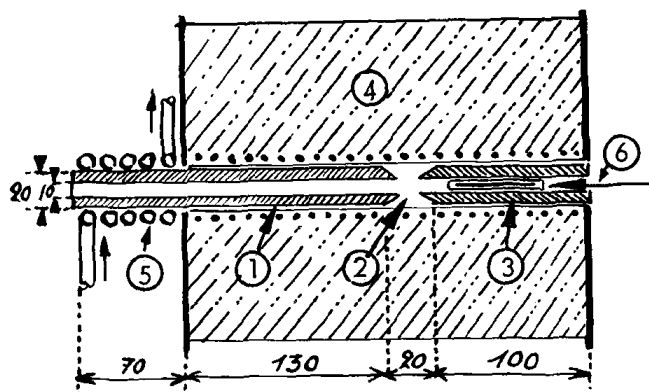


Figure 1. Shape of the temperature gradient used for the preparation of monocrystals by phase transformation. (I) $120^\circ\text{C}/\text{cm}$: samples 0.5 mm thick; (II) $70^\circ\text{C}/\text{cm}$: samples 2.3 mm thick

Original language: French.

* Centre de Recherches Métallurgiques de l'Ecole des Mines de Paris.



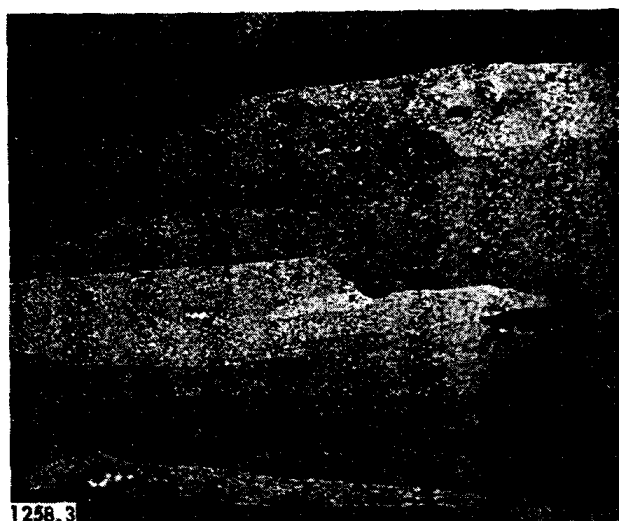
1258.2

Figure 2. Diagram of the gradient-type furnace used for the preparation of monocrystals by phase transformation. (1) Copper cylinder (very good conductor); (2) insulator (asbestos); (3) steel cylinder; (4) furnace; (5) water circulation; (6) silica plunger. The distances are given in mm

sample which is sealed in vacuum in a silica tube is not critical; it may vary from 5 to 15 cm.

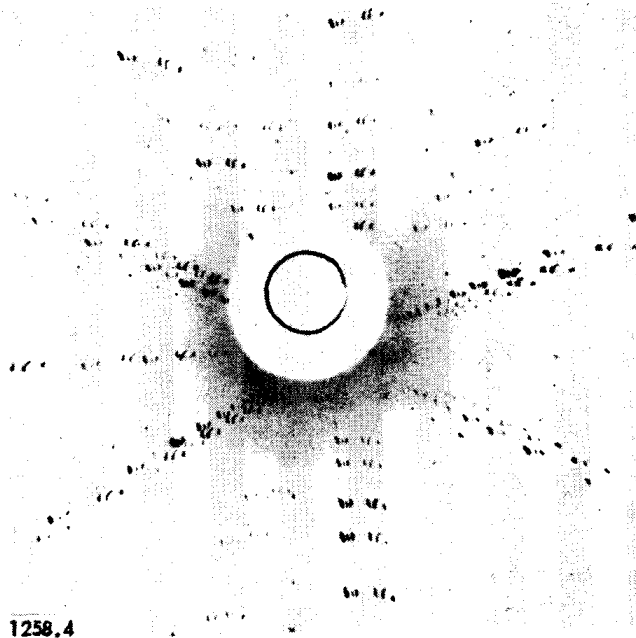
Figure 2 shows a diagram of the gradient furnace used. The horizontal arrangement has been chosen to avoid possible distortion of the samples by creeping. Finally, the composition of the metal is not critical. However, greater purity of the uranium increases the chance of success. Out of 100 processed samples, we obtained on an average 70 monocrystals and 25 bicrystals with a contour substantially parallel to the orientation of the growth.

The growth of these crystals is verified by photomicrographs and X-rays. They show a conventional "ribbon" structure, in other words, they are made of very slightly disoriented subgrains, the contours of which are essentially parallel to the direction of growth. This slight loss of orientation cannot be revealed by examination under polarized light, but is very plain after electrolytic etching⁶ (Fig. 3). X-rays show a disorientation varying from 2-10 deg maximum, according to the spread of the Laue spots, which corresponds to an irradiated area of 1 mm²



1258.3

Figure 3. Ribbon- or strip-type structure of polygonized monocrystals, produced by phase transformation, as revealed by electrolytic etching ($\times 75$)



1258.4

Figure 4. Laue diagram of the polygonized monocrystals produced by phase transformation

(Fig. 4). Therefore it is always possible to determine the orientation of imperfect crystals by Greninger's method.⁷ All orientations may be obtained and thus there is no preferential direction of growth due to the shift of the gradient.

Investigation of the Strain Deformation of the Phase-Shift Crystals

To determine the optimum conditions for the growth of perfect crystals by annealing after deformation, we made a systematic study of the types of deformation that appear when imperfect crystals are under strain, according to their orientation. In particular, a parallel study of the shape of the strain curve and of the evolution of the micrographic structure should enable us to define in a more quantitative manner the rate of cold working needed for the growth of new crystals.

As an example, we shall describe the strain curves given by a monocrystal. The first important point is obvious: The monocrystals, regardless of their orientation, always have an elastic-deformation area characterized, on the stress-strain curve, by a perfectly rectilinear and reversible tracing (Fig. 5), as shown by the load-unload cycles. On the other hand, the fine-grain polycrystalline uranium samples show no such curve.^{8,9}

The beginning of plastic deformation is indicated by the sudden change in the slope of the strain curve. Beyond that point we note, according to the type of deformation, the twinning of the crystals or deformation strips and some sudden breaks due to the violent relief of stress. These relaxations are of greater amplitude in the case of the twinned crystals (Fig. 6) than in that of the distorted strips (Fig. 7). For the most part, after the conventional corrections, the shape of the strain curve of the uranium monocrystal, allowing for the decrease in area as a function of the

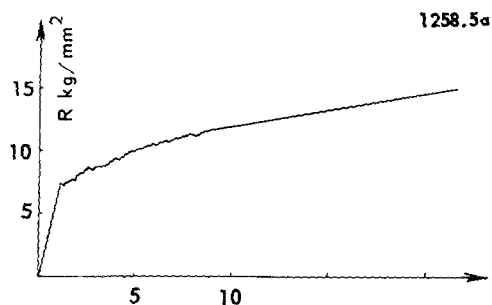


Figure 5a. Strain curve (uncorrected) of a monocrystal produced by phase transformations; the $[100]$ axis is essentially parallel to the axis of strain

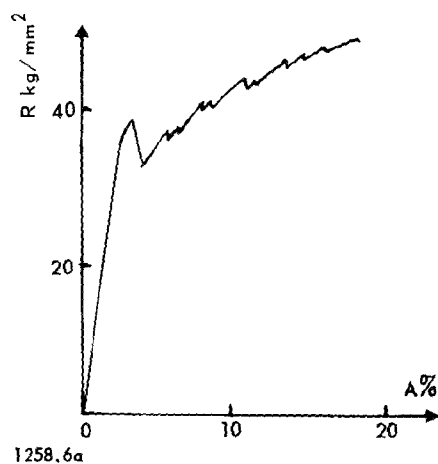


Figure 6a. Beginning of the strain curve of a monocrystal, the axis of which $[1\bar{1}5]$ coincides with the direction of strain; sudden break beyond the elastic limit due to the formation of twinned crystals

Table 1

Orientation	Elastic limit, E , kg/mm ²	Breaking load, R , kg	Elongation, $A\%$, at breaking point
$[1\bar{2}0]$	6	30	53
$[010]$	7	66	70
$[100]$	6	45	42
$[110]$	3	56	62
$[3\bar{2}4]$	6	45	43
$[041]$	25	78	43

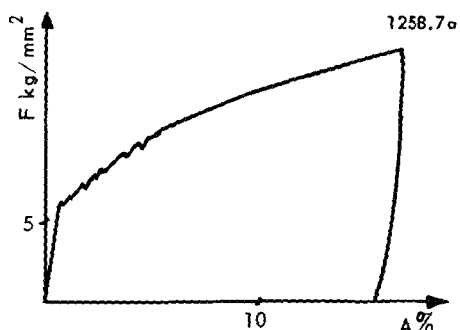


Figure 7a. Beginning of strain curve for a monocrystal with axis $[2\bar{7}4]$ parallel to the axis of strain. The successive breaks beyond the elastic limit correspond to these two deformation bands



Figure 5b. Bending deformation. The axis of strain coincides with the slip direction. Photomicrograph ($\times 150$)

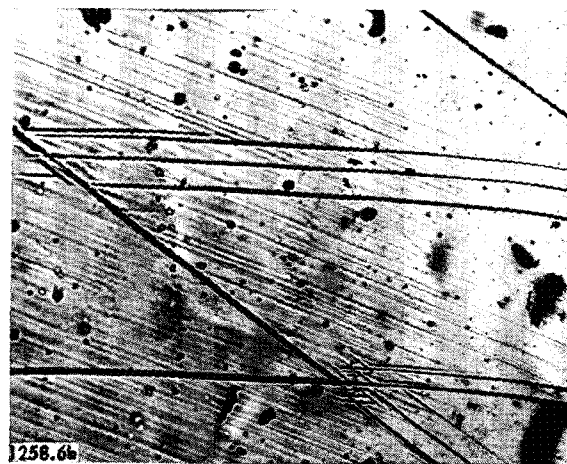


Figure 6b. Photomicrograph for the same crystal, as deformed by the formation of twin crystals and simultaneous slip ($\times 150$)

elongation, is similar to those obtained for other metals¹⁰ in a monocrystal state (Fig. 8).

The values of the mechanical parameters vary with the orientation of the monocrystal, with respect to its axis of strain. Table 1 shows a series of values of the elastic limit, the breaking load, and the elongation breaks of various crystals.



Figure 7b. Corresponding photomicrograph ($\times 150$)

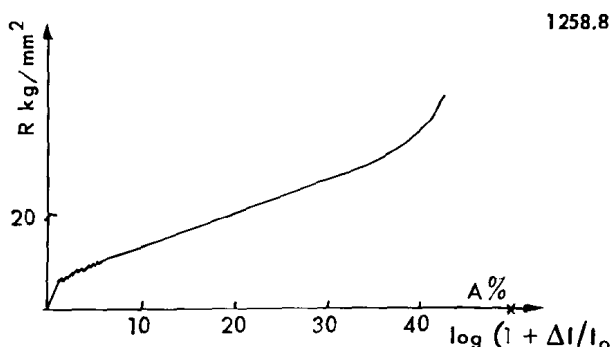


Figure 8. Complete and corrected strain curve of a monocrystal having axis $[27\bar{4}]$ parallel to direction of strain

The strain curves of bicrystalline samples, on the other hand, do not show a true elastic area and perfect reversibility of the load and unload cycles: the behavior is similar to that of the polycrystalline samples (Fig. 9). It is important to indicate that, prior to any strain, one crystal of the bicrystalline sample always has very fine twins that bear against the contour of the grain (Fig. 10). This clearly shows that, during cooling, one of the crystals has been subjected to marked stresses due to the anisotropic expansion. The stress might be considered as even greater for the fine-grain polycrystalline sample, the stresses being greater for a given grain of the aggregate where it is in contact with several crystals of different orientations. The existence of these stresses is doubtless the reason for the absence of elastic limits in polycrystalline uranium when the stress due to the anisotropy in the expansion has not been completely relieved.

In conclusion it should be noted that, on the sample polished before the load is applied, we may follow micrographically the development of the different types of distortion and relate them to the various anomalies noted in the strain curve. As shown in Fig. 11, the discontinuity *A* corresponds to the development of a few small twins (172), and *C* corresponds to that of the twins (130).

Relationship between Plastic Deformation and the Structure Obtained after Annealing above the α -Phase Range

According to the orientation and total elongation of the crystal, some slip lines, twin crystals, and de-

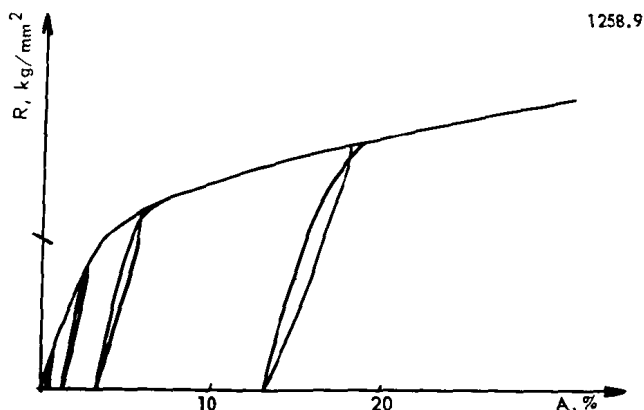


Figure 9. Strain curve for a bicrystal; absence of elastic deformation area; irreversibility of load-unload cycles

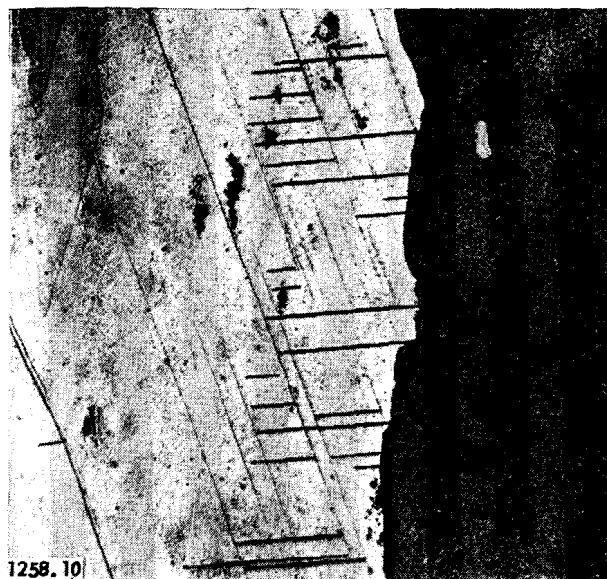


Figure 10. Formation of fine twin crystals in a single grain of the bicrystalline sample; the twin crystals stop suddenly on the joint which separates the two elements of the double crystal ($\times 75$)

formation bands develop successively or simultaneously. Thus, it is impossible to define *a priori* any critical degree of cold-working for each crystal: This will vary according to the type of deformation.

However, we may accept the classical concept of a minimum critical degree of cold-working needed for the development of new perfect crystals, by annealing, having an orientation different from that noted in the initial crystal; this is recrystallization. On the contrary, under this cold-working there will be a restoration in the sense that annealing will give an imperfect crystal but one with an orientation essentially identical with that of the initial crystal.

We shall show, by means of a few examples chosen from crystals of different orientation, how a micrographic study makes it possible to distinguish between restoration and recrystallization, according to the type of deformation undergone by the crystal prior to annealing.[†]

[†] Monocrystals have been annealed in two ways; either by suddenly bringing the temperature up to 640°C or else by shifting about in a temperature gradient that covers the whole of the α phase.

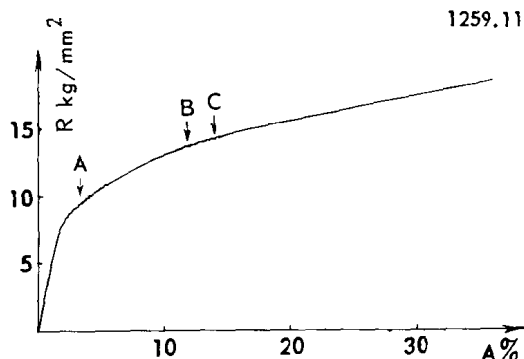


Figure 11. Analysis of the strain curve of the crystal having axis $[120]$ parallel to the direction of strain. (A) Appearance of some twin crystals; (B) critical hardening; (C) appearance of twin crystals (130)

Example of Restoration

This restoration seems to be possible regardless of the deformation method (twinning, bending or slipping) provided the cold working, as defined by the total elongation of the crystal, is small.

(a) *Example of slip or deformation of the bands.* For small elongations deformation bands appear when the axis of deformation is perpendicular to the direction of slip [010] (Fig. 5) and sometimes in the direction of slip. In the first case, there is a rotation of the lattice around the [001] axis, perpendicular to the direction of the slip, and located in the plane of slip. This is shown by the large Laue diagram in Fig. 12, in which the spot corresponding to the [001] axis has not changed.

Figure 13 shows the micrographic aspect of a bundle of fine deformation bands which are distinct from one another. After annealing at 640°C, these give rise to a polygonized structure, the subunits of which are essentially parallel to the longitudinal direction of the deformation bands. This polygonized structure is superimposed on the "ribbon" structure, which is the initial one noted in the phase-change crystal. Polygonization of the area of the crystal that is primarily covered with intertwined deformation bands would be due to the disappearance of the curvature of the slip planes that define the boundary of each band at its contact with the parent crystal.

(b) *Example of deformation by twinning.* For small elongations (about 2%) variable according to the orientation of the crystal, the phase-change crystals, deformed only by twinning of the crystals, can be completely restored so that there is complete absorption of the twinning during annealing. This behavior is similar to that of the twinned titanium¹¹ or magnesium crystals.¹²

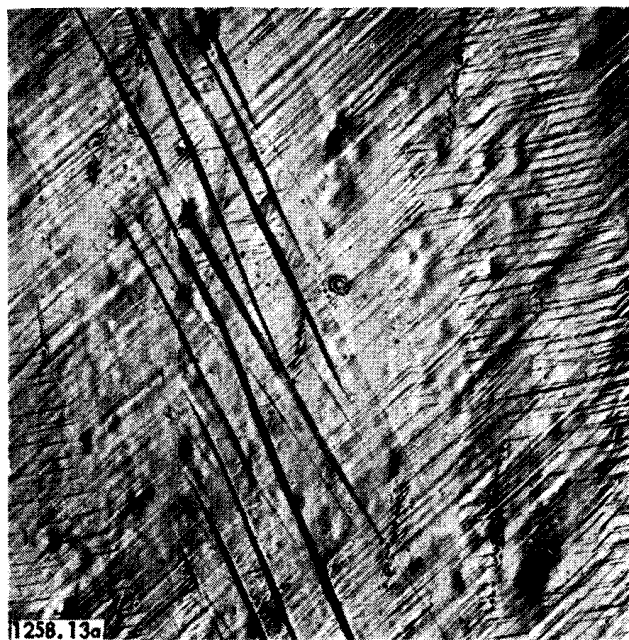


Figure 13a. Phase-change monocrystal under strain; note the deformation bands on the polished surface ($\times 150$)

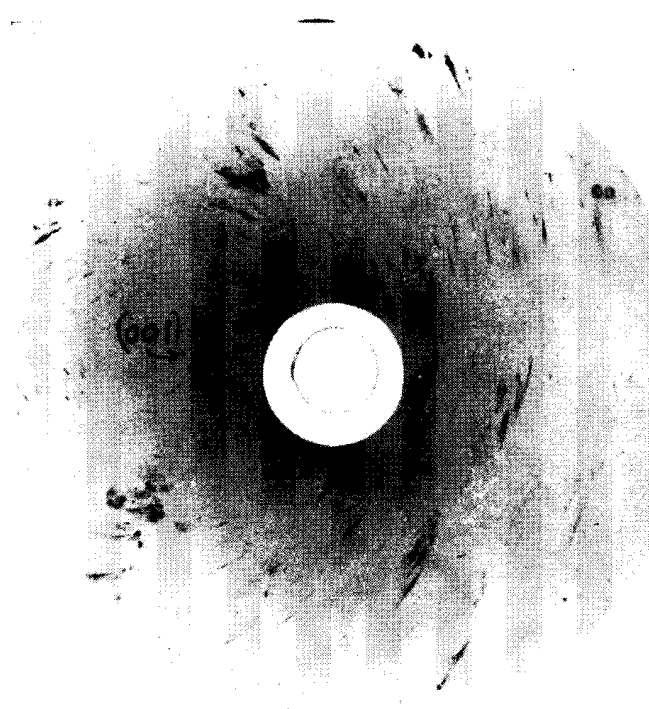


Figure 12. Laue diagram for a monocrystal, with a strain of 4% along the axis [221] annealed 50 hr at 640°C; rotation of lattice around axis [001]

For larger elongations, where there are many fine nearly equidistant twinned crystals (Fig. 14) that cover the whole volume of the crystal, the restoration is accompanied by an absorption of some parts of the twinned crystals while others become wider (Fig. 15). A second proof of the restoration is shown by the persistence of a polygonized structure at whose joints the extremities of the twinned crystals, as widened by the annealing, come to bear (Fig. 15).

For some orientations, deformation by twinning is limited to the development of very fine and very short



Figure 13b. The same area after annealing for 50 hr at 640°C. Superimposition of two polygonization lattices; one corresponds to the initial polygonization of the crystal, the second to the polygonization of the deformation bands

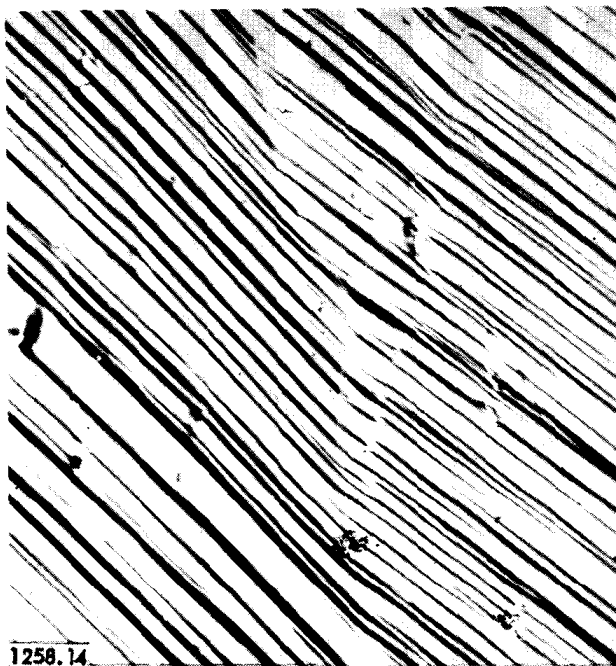


Figure 14. Fine equidistant twin crystals which appear after 2% strain of an imperfect monocrystal at the phase change ($\times 150$)

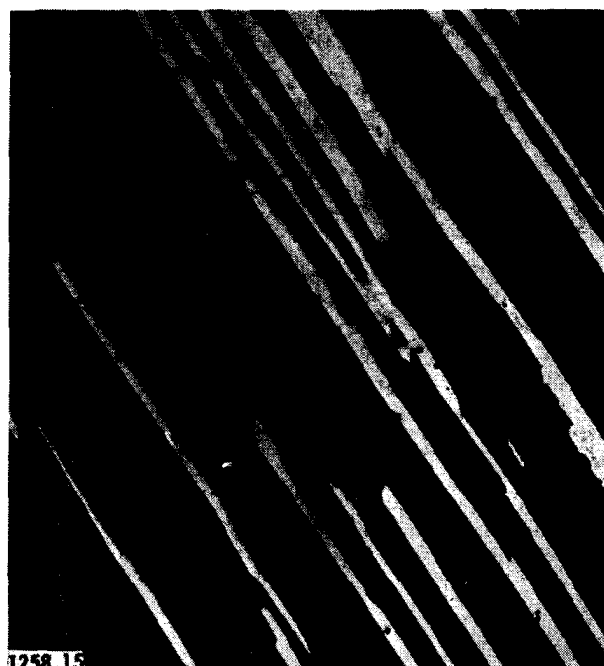


Figure 15. Same area following restoration annealing; there remain polygonization strips against which a small number of enlarged twin crystals come to bear ($\times 150$)

twin crystals that arise out of the subjoinths of the polygonized structure (Fig. 16). If the deformation is sufficient, these short twinned crystals are very numerous and very tightly packed so that, during subsequent annealing at 640°C , they appear to coalesce to give a crystal elongated in the direction of the subjoinths. We are dealing, in fact, with a polygonized crystal the edges of which remain very pronounced as they follow the initial shape of the extremities of the small twins (Fig. 17). It would seem, in this case, that we are dealing with a true recrystallization, generated by these fine twinned crystals, rather than a restoration.

(c) *Example of slip deformation.* For some orientations of the initial crystal, the deformation causes a simultaneous appearance of slip lines and twins: The slip is preponderant so that, as elongation increases, there is a progressive rotation of the crystal with respect to the direction of the strain. With annealing at 640°C , the twins disappear completely and there is polygonization of the crystal with subjoinths essentially perpendicular to the slip lines. This polygonization due to annealing does not eliminate the "ribbon" structure of the first crystal and thus there are two lattices of superimposed subjoinths (Fig. 18) as in the case of annealing the deformation bands (Fig. 13).

Examples of Recrystallization

For larger degrees of instability than those which gave restoration, annealing causes the appearance of recrystallization, where the orientation is homogeneous throughout the volume. The relationships between the deformation structure and recrystallization will be described below.

(a) *Case of deformation by deformation bands.* For an imperfect crystal with the beginning of the orientation that fulfils the conditions mentioned

above, we see, by annealing at 640°C , either a recrystallization of part of the sample or complete recrystallization.

The distribution of the deformation bands due to strain in a monocrystal is far from being homogeneous, even when the total elongation of the crystal is greater than that which leads to restoration by subsequent annealing. Consequently, the appearance of new recrystallization crystals remains localized in the crystal volume affected by the deformation bands (Fig. 19). The crystals so created show a high degree of perfection, according to the appearance of the spots on the Laue back-reflection diagram (Fig. 20). However, if the regions covered by the deformation bands are separa-

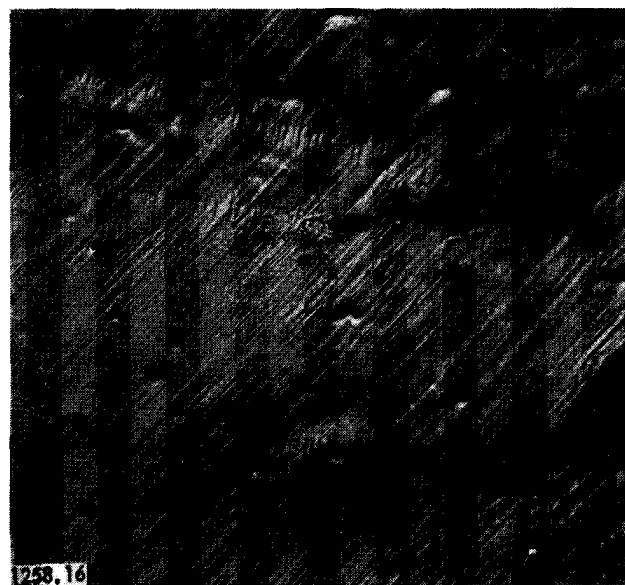


Figure 16. Development of fine and short twin crystals along the subjoinths of an imperfect phase-shift monocrystal following 3% strain, ($\times 150$)



Figure 17a. After annealing at 640°C there is a recrystallization process along the same subgrains ($\times 150$)



Figure 17b. Balance of highly polygonized crystals along the old subgrains following 6% hardening and annealing ($\times 150$)

ted from each other by undistorted areas, the crystals formed above the deformation bands will have very similar orientation. Quite often, it is possible to deduce their orientation from that of the initial matrix by a simple rotation. We shall give two examples of the growth of perfect crystals in the deformation bands: A monocrystal having an axis $[0\bar{3}4]$ perpendicular to the direction of slip $[100]$ led to the development of three distinct crystals along the deformation bands. Two of them have the same orientation $(211) [\bar{1}\bar{2}0]$,[‡] while the third has an orientation $(221) [\bar{3}\bar{3}1]$, which is very close to the first

[‡] The orientation is defined by the crystalline plane parallel to the surface and by the direction parallel to the longitudinal direction.

two since it can be produced from them by a 6 deg rotation about the $[20\bar{3}]$ axis (Fig. 21). On the other hand, it is not possible to establish a simple connection between the orientation of these recrystallization crystals and the original or parent crystal. Secondly, a monocrystal, having an axis $[\bar{2}21]$ and elongated 5%, is distorted by deformation bands. Annealing shows the development of two crystals with similar orientations, namely, $(104) [\bar{4}\bar{2}1]$ and $(117) [\bar{4}\bar{1}1]$, which can be deduced one from the other by a rotation of 73 deg about the $[230]$ axis. In this instance it is possible to relate the orientation of the recrystallization crystals to that of the parent crystal by a simple rotation about axis $[10\bar{3}]$, close to axis $[001]$, and located in the slip plane (Fig. 22).

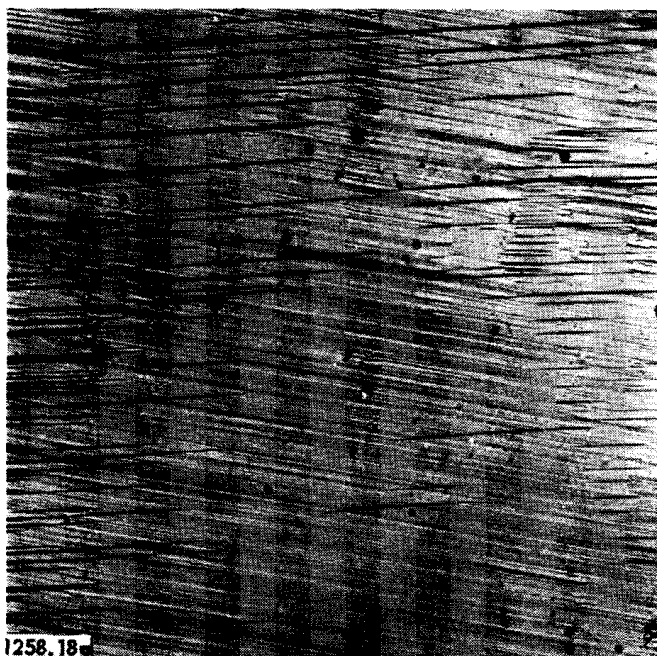


Figure 18a. Slip deformation and twin crystals of a 3% hardened phase-shift monocrystal ($\times 150$)



Figure 18b. The same crystal after 50 hr of annealing at 640°C; there is a restoration which leads to the superimposition of two polygonizing lattices ($\times 150$)



Figure 19. The same imperfect crystal, as hardened by strain, gives after annealing a recrystallization crystal, R, which develops along the distortion strips, and an imperfect serrated-contour crystal, P, at the level of the short twin crystals formed on a subgrain of the original crystal ($\times 40$)

It would seem, therefore, that total recrystallization of the original monocrystal into a single perfect crystal might be obtained if the deformation bands could be developed uniformly all along the strained sample. The growth of a perfect single crystal would be further facilitated by continuous displacements of the sample in a temperature gradient without, of course, exceeding the transformation temperature of $\beta \rightarrow \alpha$.

(b) *Example of deformation due to twinning.* Some recrystallization crystals generally develop starting from the intersections of twinning crystals that are areas of considerable deformation (Fig. 23).

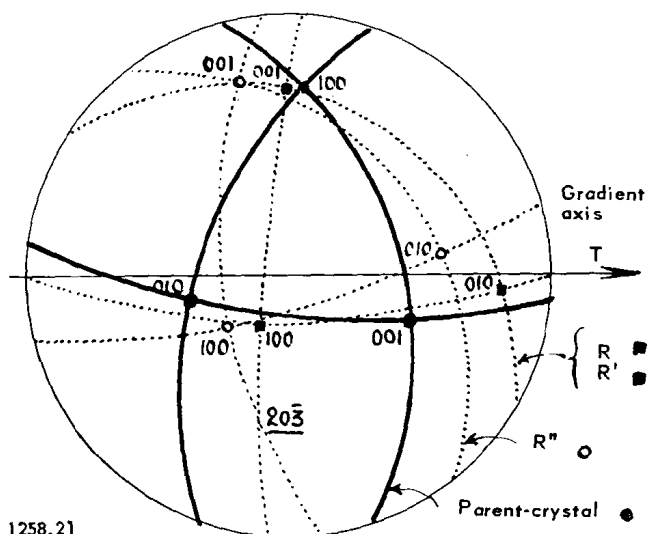


Figure 21. Stereographic projection (with respect to the plane of the sample) of the orientations of the 3 recrystallization crystals developed from deformation bands; R and R' have similar orientations, and R'' has an orientation produced from R and R' by rotation about axis $[20\bar{3}]$

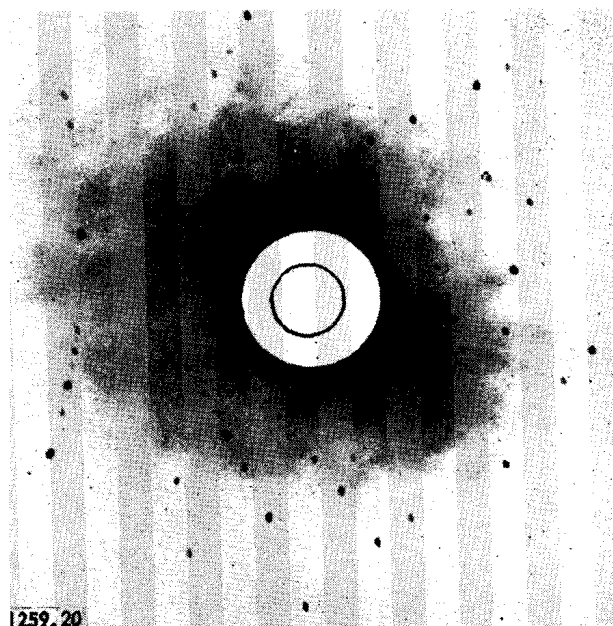


Figure 20. Laue back-reflection diagram corresponding to perfect crystal, R, excluding the fine twin crystals developed on cooling after annealing

It is also possible to observe the development of crystals due to local twinning, where plastic deformation has created essentially a single system of twin crystals (Fig. 24). If this local enlargement is developed parallel to the rectilinear outline of the twin crystals it might be the cause of their thickening, as mentioned above, for a small deformation. For larger plastic deformation, this thickening might lead to coalescence of several neighboring crystals with the same orientation in this single sheet (Fig. 25). It is difficult, in such a case, to say whether one is dealing with a true recrystallization, or restoration as defined in Fig. 15.

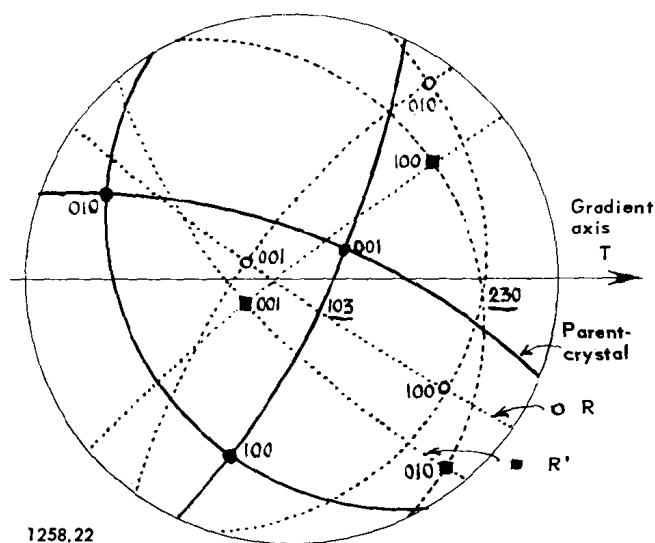


Figure 22. Stereographic projection (with respect to the plane of the sample) of two recrystallization crystals R and R', developed from deformation bands; the orientation of one is produced from that of the other by rotation around axis $[230]$, which is common to both. The orientation of R and R' may be produced from that of the parent crystal by rotation about axis $[10\bar{3}]$